International Journal of Microwave and Wireless Technologies, 2014, 6(6), 581–590.
doi:10.1017/S1759078714000257

RESEARCH PAPER

Laser induced microwave oscillator under the influence of interference

ARINDUM MUKHERJEE[1], SOMNATH CHATTERJEE[2], NIKHIL RANJAN DAS[3] AND BAIDYANATH BISWAS[4]

An optoelectronic oscillator (OEO) under the influence of a weak interference has been investigated. The system equation of the OEO under the influence of interference has been derived. A novel technique for calculating the lock range of the oscillator using the harmonic balance method in presence of interference has been demonstrated. Theoretical analysis coupled with experimental results has been presented.

Keywords: Optoelectronic oscillator (OEO), Mach–Zehnder modulator, Interference, Lock range

Received 24 October 2013; Revised 2 February 2014; first published online 18 March 2014

I. INTRODUCTION

Optoelectronic oscillator (OEO) was first proposed by M Nakazawa, T Nakashima, and M Tokuda [1] in 1984 the journey of Optoelectronic oscillator (OEO) in shown in Fig. 1. The configuration of an OEO is similar to that of the van der Pol oscillator. In the van der Pol oscillator, the flux of electrons from the cathode to the anode is controlled by the potential on the inverting grid and thus this potential is affected by the feedback current in the anode circuit comprising a tuned circuit Fig. 2.

A van der Pol oscillator can be converted to an OEO by replacing the function of electrons by photons, the function of the grid by an electrical–optical (E/O) converter, the function of the anode by an optical–electrical (O/E) converter, and finally the energy-storage function of the LC circuit by a long optical delay line.

The structure of the Laser Induced Microwave Oscillator (LIMO) is described in Fig. 2. Here, light from an E/O modulator is detected by a photo detector after passing through a long optical delay line which is then amplified and fed back to the electrical port of the E/O modulator. If the modulator is properly biased and the small signal loop gain is larger than unity, self-sustained oscillations are achieved [2–7]. The optical output of the intensity modulator is then passed down a long optical fiber delay line and into a photodiode. The recovered electrical signal is amplified and passed through an electronic bandpass filter. The output of the filter is then connected to the RF input of intensity modulator in order to complete the optoelectronic cavity. The electronic bandpass filter selects the frequency of oscillation by attenuating the other free-running modes below threshold [2–5]. The use of the very low loss optical fiber delay line is to create a cavity with a very high Q factor. The Q factor can be defined as the ratio of the stored energy in the cavity over the loss of the cavity. Since the loss of the fiber delay line is on the order 0.2 dB/km, a very long fiber can store a large amount of energy with very little loss. Because of this the Q factor of the OEO can easily achieve the level of 10^6 or

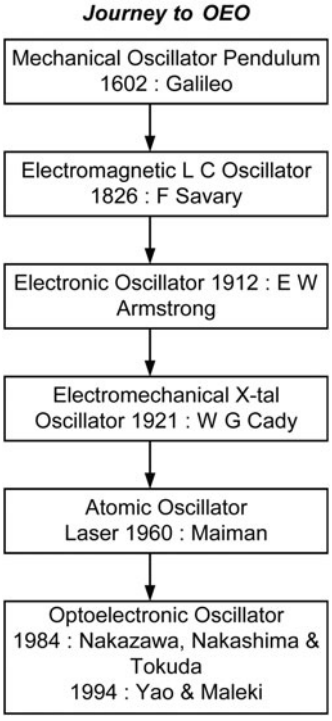

Fig. 1. Journey to OEO.

[1]Department of Electronics and Communication Engineering, Central Institute of Technology, Kokrajhar, Assam 783370, India
[2]Kanailal Vidyamandir (French Section), Chandernagore, India. Phone: +919433981389
[3]Institute of Radiophysics and Electronics, Calcutta University, 92 A.P.C. Road, Kolkata 700009, West Bengal, India
[4]Education Division, SKF Group of Institution, Mankundu, Hooghly 712139, West Bengal, India
Corresponding author:
S. Chatterjee
Email: somnathchat@yahoo.com

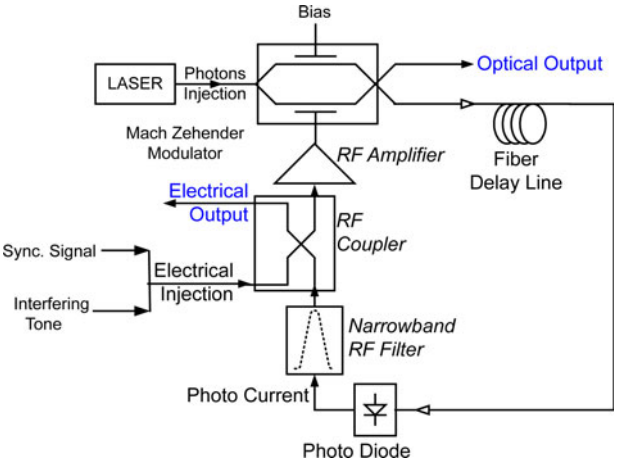

Fig. 2. Optoelectronic oscillator with interference.

higher. Yao and Maleki [6] have developed a quasi-linear theory for the threshold condition, the amplitude, the frequency, the line width, and the spectral power density of the oscillation in OEO. The long delay line used in the oscillator can, however, support many modes of oscillation. Mode spacing is inversely proportional to the delay length of the optical link. The oscillator Q can be improved by increasing the delay length at the expense of tighter mode spacing. The undesirable modes become more difficult to filter in the RF domain as the spacing becomes closer [7–11]. The stability analysis of LIMO has been studied using Barkhausen criteria by Biswas *et al.* [12]. The effect of interfering signal on a synchronized oscillator has been studied in detail by earlier workers [13–15]. The contribution of phase noise in a multiloop OEO has been investigated [16] and the movement of poles in OEO has been analyzed by Chatterjee *et al.* [17].

As the technology has advanced, OEOs have been demonstrated to generate RF signals at frequencies starting in the microwave range and extending out to the millimeter wave range. Work continues on improving the performance of the original OEO, from using multiple loops to suppress the non-oscillating side modes by removing the bandpass filter in order to tune the frequency of RF output [18, 19]. Further work has been done on improving the phase noise performance by removing the electronic amplifier from the cavity while also looking at miniaturizing the OEO for use in satellites and computers. In terms of digital optical networks, the OEO has been used for both data clock recovery as well as data format conversion. Demonstrations of the OEO continue to explore new applications, from generating broadband chaos [20], use in sensors [21], performance evaluation utilizing photonic crystal fiber and standard fibers as delay lines [22], and as a measurement of the refractive index of optical fibers [23].

If a sinusoidal signal acts on a nearly sinusoidal oscillator then the behavior of the oscillator affects in many aspects depending on the strength and frequency of the forcing signal. A forcing signal when injected into an oscillator modifies its properties in many ways. Within the synchronization range the locked oscillator loses its identity and obeys command from the forcing signal, and the oscillator is said to be injection locked (phase locked) to the synchronization signal [12–15]. It is to be noted that the forcing signal can be injected into the OEO as an electrical or optical synchronizing signal. However, for the present study, we have considered the forcing synchronizing signal to be in the electrical form.

In this paper, we have derived an expression for the locking-range of an OEO under the influence of weak interference. We also show the variation of locking-range with injection amplitude. Finally, the effect of frequency-pulling and pushing on locking-range is also observed when the interference is swept away from the OEO's center frequency.

II. SYSTEM EQUATION OF OEO IN PRESENCE OF INTERFERENCE

Let the RF input to the modulating grid of the Mach–Zehnder modulator (MZM) is given by

$$v_{in}(t) = V(t)e^{j[\omega_1 t+\theta(t)]};$$

the synchronizing signal to be $S(t) = Ee^{j\omega_i t}$ and the interfering tone to be $I(t) = yEe^{j\omega_i t}$, where "ω_i" is the interfering frequency which is lying away from the OEO's free-running frequency, "y" is the fraction which indicates the strength of the interfering tone with respect to synchronizing signal, and "$\Delta\omega = \omega_1 - \omega_i$" is the de-tuning frequency. If "$G(s)$" is the transfer function of the RF tuned circuit, then it can be expressed as [14] $1/G(s) = 1 + Q((s/\omega_o) + (\omega_o/s))$, where "$Q$" is the quality factor of the tank circuit.

To analyze the behavior of the OEO in presence of the interfering signal shown in Fig. 2, we will assume that the OEO, instead of being exposed simultaneously to both the synchronizing signal and the interfering tone, is initially locked to the synchronizing signal and then it is influenced by the interfering tone which does not throw the system out of synchronism. In this condition, the instantaneous phase of the OEO will fluctuate around the static phase error "θ_1" at a rate depending upon the difference of frequencies between the synchronizing signal and the interfering tone. Similarly, the amplitude of the forced oscillator will also vary around the steady state value at a rate depending upon the frequency difference between the two signals. The static phase error "θ_1" gives a measure of the initial detuning of the OEO with respect to the synchronizing signal [15].

Now, in order to find the system equation of the OEO in presence of interference we assume that despite the presence of strong non-linearity of MZM, there exists stationary amplitude of the microwave oscillation [12] of the form

$$v_{in}(t) = V(t)\exp(j\omega t + \theta(t)).$$

The output power [7, 17] of the MZM can be expressed as

$$P(t) = \frac{1}{2}\alpha P_o\left[1 - \eta\sin\left(\frac{v_{in}(t) + V_B}{V_\pi}\right)\right];$$

where "α" is the fraction of insertion loss of the modulator, "V_π" is the half-wave voltage, "V_B" is the bias voltage, "P_o" is the input optical power, "$v_{in}(t)$" is the input RF voltage to the modulator and, "η" determines the extinction ratio of the modulator. Therefore, the output voltage of the photo

https://doi.org/10.1017/S1759078714000257 Published online by Cambridge University Press

detector when the output of the MZ modulator shines on it is

$$\begin{aligned} V_o(t) &= \rho Z_{ph} P(t-\tau) \\ &= \rho\sqrt{R^2+\frac{1}{\omega^2C^2}}P(t-\tau)e^{-j\tan^{-1}\left(\frac{1}{\omega CR}\right)} \\ &\cong \rho RP(t-\tau)e^{\frac{1}{j\omega\tau_1}}; \end{aligned}$$

where "ρ" is the sensitivity, "$Z_{ph} = R - (j/\omega\, C)$" is the output impedance of the photo-detector and "$\tau_1 = RC$" is the time-constant of photo-detector. Hence using the above arguments, it is not difficult to show that the output of the MZM [12] can be expressed as

$$\begin{aligned} V_o(t) &= -2\eta V_{ph}\cos\left(\frac{\pi V_B}{V_\pi}\right)J_1\left(\frac{\pi V(t-\tau)}{V_\pi}\right) \\ &\quad\times \sin[\omega(t-\tau)]e^{\frac{1}{j\omega\tau_1}} \\ &= \frac{N(V(t-\tau))}{V}\exp(-s\tau)v_{in}(t)\exp\left(\frac{1}{s\tau_1}\right) \end{aligned}$$

where,

$$N(V(t-\tau)) = -2\eta V_{ph}\cos\left(\frac{\pi V_B}{V_\pi}\right)J_1\left(\frac{\pi V(t-\tau)}{V_\pi}\right) \text{ and}$$

$$V_{ph} = \frac{\rho R\alpha P_o}{2}.$$

Thus, the closed-loop equation of the OEO in presence of injection is given by

$$\left[\frac{N(V(t-\tau))}{V}e^{-s\tau}e^{\frac{1}{s\tau_1}}v_{in}(t) + Ee^{j\omega_1 t} + yEe^{j\omega_i t}\right] = \frac{v_{in}(t)}{G.G(s)}. \quad (1)$$

$$\left[\frac{N(V(t-\tau))}{V}e^{-s\tau}e^{\frac{1}{s\tau_1}} + \frac{E}{V}e^{-j\theta(t)} + y\frac{E}{V}e^{-j[\Delta\omega t+\theta(t)]}\right]v_{in}(t) = \frac{v_{in}(t)}{G.G(s)}. \quad (2)$$

Again, the complex frequency can be written as [12]

$$\left.\begin{aligned} s = j\omega &= \frac{1}{v_{in}(t)}\frac{dv_{in}(t)}{dt} = \frac{1}{V(t)}\frac{dV(t)}{dt} + j\left(\omega_1 + \frac{d\theta}{dt}\right) \\ \frac{1}{j\omega} &\cong \frac{1}{j\omega_1} + \frac{1}{\omega_1^2}\left(\frac{1}{V(t)}\frac{dV(t)}{dt} + j\frac{d\theta}{dt}\right) \end{aligned}\right\}. \quad (3)$$

Rewriting (2) with the help of (3)

$$\begin{aligned} &N(V(t-\tau))e^{-j\omega_1\tau}e^{\frac{1}{j\omega_1\tau_1}} + Ee^{-j\theta(t)} + yEe^{-j[\Delta\omega t+\theta(t)]} \\ &= \left(\frac{V}{G}\right)\left[1 + \frac{Q}{V}\left(\frac{1}{\omega_0}+\frac{\omega_0}{\omega_1^2}\right)\frac{dV}{dt} + jQ\left\{\left(\frac{\omega_1}{\omega_0}-\frac{\omega_0}{\omega_1}\right)\right.\right. \\ &\left.\left. + \left(\frac{1}{\omega_0}+\frac{\omega_0}{\omega_1^2}\right)\frac{d\theta}{dt}\right\}\right]. \end{aligned} \quad (4)$$

Under the assumption that $V_B = V_\pi$, $\eta = 1$, $\pi V_{ph} = V_\pi$ and $V_\pi = \pi$ [12], we have $N[V(t-\tau)] = 2J_1[V(t-\tau)]$ and when $\omega_1 \approx \omega_o$, the real part of equation (4) gives the amplitude equation as

$$\begin{aligned} \frac{dV}{dt} &= \left(\frac{\omega_0}{2Q}\right)\left\{2GJ_1[V(t-\tau)]\left\{\cos(\omega_0\tau) + \frac{\sin(\omega_0\tau)}{\omega_0\tau_1}\right\} - V\right\} \\ &\quad + \left(\frac{\omega_0}{2Q}\right)GE\{\cos(\theta) + y\cos(\Delta\omega t+\theta)\}. \end{aligned} \quad (5)$$

Similarly equating the imaginary part, the phase equation can be obtained as

$$\begin{aligned} &2J_1[V(t-\tau)]\left\{\sin(\omega_1\tau) - \frac{\cos(\omega_1\tau)}{\omega_1\tau_1}\right\} + E\{\sin(\theta(t)) \\ &\quad + y\sin(\Delta\omega t+\theta(t))\} = -\left\{\frac{QV}{G}\left[\left(\frac{\omega_1}{\omega_0}-\frac{\omega_0}{\omega_1}\right)\right.\right. \\ &\quad \left.\left. + \left(\frac{1}{\omega_0}+\frac{\omega_0}{\omega_1^2}\right)\frac{d\theta}{dt}\right]\right\}. \end{aligned} \quad (6)$$

Again for $\omega_1 \approx \omega_o$, the phase balance equation can be rewritten as

$$\begin{aligned} \frac{d\theta}{dt} &= (\omega_o - \omega_1) - \left(\frac{\omega_0}{2Q}\right)\left[\frac{2GJ_1[V(t-\tau)]}{V}\left\{\sin(\omega_0\tau)\right.\right. \\ &\quad \left.\left. - \frac{\cos(\omega_0\tau)}{\omega_0\tau_1}\right\}\right] - \left(\frac{\omega_0}{2Q}\right)\left[\left(\frac{GE}{V}\right)\{\sin(\theta(t)) \right. \\ &\quad \left. + y\sin(\Delta\omega t+\theta(t))\}\right]. \end{aligned} \quad (7)$$

The photo-detector impedance "R" is replaced by "$R - (j/\omega C)$" but it has no effect in our chosen frequency range. The effect of incorporating the photo-detector impedance in the amplitude and phase equations (5) and (7) has not been reported by other authors also.

III. WEAK INTERFERENCE LYING AWAY FROM THE OEO'S FREE-RUNNING FREQUENCY

Let us assume the solution for (6) as

$$\theta = \theta_1 + m\sin(\Delta\omega t + \alpha), \quad (8)$$

https://doi.org/10.1017/S1759078714000257 Published online by Cambridge University Press

where "θ_1" is the steady-state phase error, and the modulation index is small for low-level interference. Using (8) in (7), we get

$$\begin{aligned} & m\Delta\omega\cos(\Delta\omega t+\alpha) \\ & = (\omega_o-\omega_1)-\left(\frac{\omega_o}{2Q}\right)\left[\frac{2GJ_1[V(t-\tau)]}{V}\right. \\ & \left.\left\{\sin(\omega_o\tau)-\frac{\cos(\omega_o\tau)}{\omega_o\tau_1}\right\}\right]-\left(\frac{\omega_o}{2Q}\right)\left(\frac{GE}{V}\right) \\ & \times\begin{bmatrix} J_o(m)\sin\theta_1+2J_1(m)\cos\theta_1\sin(\Delta\omega t+\alpha) \\ +yJ_o(m)[\sin\theta_1\cos(\Delta\omega t)+\cos\theta_1\sin(\Delta\omega t)] \\ +yJ_1(m)[\cos\theta_1\sin\alpha-\cos\alpha\sin\theta_1] \end{bmatrix}. \end{aligned} \tag{9}$$

Using harmonic balance method [15], we get

$$\begin{aligned} & 2Q\left(\frac{\omega_1-\omega_o}{\omega_o}\right)=\Omega \\ & =-\left[\frac{2GJ_1[V(t-\tau)]}{V}\left\{\sin(\omega_o\tau)-\frac{\cos(\omega_o\tau)}{\omega_o\tau_1}\right\}\right] \\ & -\left(\frac{GE}{V}\right)\left[J_o\left(m\right)\sin\theta_1+yJ_1\left(m\right)\sin(\alpha-\theta_1)\right]. \end{aligned} \tag{10}$$

Similarly, denoting $p=\left(\frac{\omega_o}{2Q}\right)\left(\frac{GE}{V}\right)$.

$$\frac{m\Delta\omega}{p}\cos\alpha=-\left[2J_1(m)\cos\theta_1\sin\alpha+yJ_o(m)\sin\theta_1\right],$$

and

$$\frac{m\Delta\omega}{p}\sin\alpha=2J_1(m)\cos\theta_1\cos\alpha+yJ_o(m)\cos\theta_1. \tag{11}$$

Hence, it is not difficult to show using (11) that

$$\sin(\alpha-\theta_1)=\frac{m\left(\Delta\omega/p\right)}{yJ_o(m)}. \tag{12}$$

Substituting the value of (12) in (10)

$$\begin{aligned} \Omega & =-\left[\frac{2GJ_1[V(t-\tau)]}{V}\left\{\sin(\omega_o\tau)-\frac{\cos(\omega_o\tau)}{\omega_o\tau_1}\right\}\right] \\ & -\left(\frac{GE}{V}\right)\left[J_o(m)\sin\theta_1+\left(\frac{m\Delta\omega}{p}\right)\frac{J_1(m)}{J_o(m)}\right]. \end{aligned} \tag{13}$$

Again, using (11), it is not difficult to show that

$$\begin{aligned} \Omega & =-\left[\frac{2GJ_1[V(t-\tau)]}{V}\left\{\sin(\omega_o\tau)-\frac{\cos(\omega_o\tau)}{\omega_o\tau_1}\right\}\right]-\left(\frac{GE}{V}\right) \\ & \times\left[J_o(m)\sin\theta_1+\frac{m\left(\Delta\omega/p\right)y^2J_o(m)J_1(m)}{m^2\left(\Delta\omega/p\right)^2+4J_1^2(m)\cos^2\theta_1}\right]. \end{aligned} \tag{14}$$

Now, for low-level interference, "m" is small and $J_o(m)\cong 1$; $J_1(m)\cong m/2$. Maximum value of "θ_1" is $\pm(\pi/2)$. Hence from (14)

$$\begin{aligned} \Omega & =-\left[\frac{2GJ_1[V(t-\tau)]}{V}\left\{\sin(\omega_o\tau)-\frac{\cos(\omega_o\tau)}{\omega_o\tau_1}\right\}\right] \\ & -\left(\frac{GE}{V}\right)\left[\sin\theta_1+\left(\frac{y^2}{2}\right)\frac{\left(\Delta\omega/p\right)}{\left(\Delta\omega/p\right)^2+\cos^2\theta_1}\right] \\ & =-\left[\frac{2GJ_1[V(t-\tau)]}{V}\left\{\sin(\omega_o\tau)-\frac{\cos(\omega_o\tau)}{\omega_o\tau_1}\right\}\right] \\ & -\left(\frac{GE}{V}\right)\left[\pm 1+\frac{y^2/2}{\left(\Delta\omega/p\right)}\right]. \end{aligned} \tag{15}$$

Now, $\frac{y^2}{2}\frac{p}{\Delta\omega}$ can be written as $\frac{y^2}{2}\frac{p}{\Delta\omega}=\Delta\omega-\sqrt{(\Delta\omega)^2-y^2p}$. Thus, the lock-range of the OEO in presence of the interfering tone is given by

$$\begin{aligned} \Omega & =-\left[\frac{2GJ_1[V(t-\tau)]}{V}\left\{\sin(\omega_o\tau)-\frac{\cos(\omega_o\tau)}{\omega_o\tau_1}\right\}\right] \\ & -\left(\frac{GE}{V}\right)\left[1+\left(\Delta\omega-\sqrt{(\Delta\omega)^2-y^2p}\right)\right]. \end{aligned} \tag{16}$$

In deriving the steady-state value for the lock range given by equation (16), the positive sign of (15) has been considered. Moreover, since "$V(t)$ and $\theta(t)$" are slowly varying functions of time [14], i.e. $\frac{1}{\omega_o}\left(\frac{d\theta}{dt}\right)\ll 1$ and $\frac{1}{V}\left(\frac{dV}{dt}\right)\ll 1$,

$$V(t-\tau)\approx V(t)-\tau\frac{dV}{dt}\approx V(t)\left[1-\frac{\tau}{V}\frac{dV}{dt}\right]\approx V(t),$$

and thus in the steady state $J_1[V(t-\tau)]\approx J_1[V(t)]\simeq\frac{V(t)}{2}$.

From (15), it is clear that in absence of interference

$$\Omega|_{Lower}=-\left[\frac{2GJ_1[V(t-\tau)]}{V}\sin(\omega_o\tau)\right]-\left(\frac{GE}{V}\right)\Big|_{\theta_1=+\frac{\pi}{2}}. \tag{17}$$

$$\Omega|_{Upper}=-\left[\frac{2GJ_1[V(t-\tau)]}{V}\sin(\omega_o\tau)\right]+\left(\frac{GE}{V}\right)\Big|_{\theta_1=-\frac{\pi}{2}}. \tag{18}$$

Hence $\Omega_{Lower}>\Omega_{Upper}$, which is also confirmed from the experimental findings given in Table 1 and Fig. 8. This asymmetric nature of the locking range of an OEO has not been reported so far as far as the knowledge of the authors goes.

https://doi.org/10.1017/S1759078714000257 Published online by Cambridge University Press

Table 1. Locking range with fiber delay.

Delay (μs)	Lower locking range (MHz)	Upper locking range (MHz)	Lower lock range w.r.t free running (kHz)	Upper lock range w.r.t free running (kHz)
1.0	11.949	12.051	−53.0	49.0
3.0	11.9695	12.031	−32.5	29.0
5.0	11.978	12.022	−24.0	20.0
7.0	11.983	12.017	−19.0	15.0
10.0	11.988	12.012	−14.0	10.0

Laser frequency = 500 Mrad/s; free-running frequency = 12.002 MHz; RF gain = 3; synchronizing signal strength = 0.4 V; interfering signal strength = 0 V.

IV. RESPONSE OF OEO TO NOISY SIGNAL

Thermal noise is the unavoidable form of interference that affects the behavior of the closed-loop system shown in Fig. 4. The power spectral density of the thermal noise is flat, frequency independent and hence the name white noise. It is expedient to write the signal contaminated with additive white Gaussian noise while passing through the narrow-band tuned circuit in absence of interfering tone as

$$v_n(t) = \sqrt{2}\, V_C(t)\cos[\omega_1 t + \theta(t)] + \sqrt{2}\, V_S(t)\sin[\omega_1 t + \theta(t)]$$
$$= \sqrt{2\left[V_C^2(t) + V_S^2(t)\right]}\, e^{j[\omega_1 t + \theta(t) - \theta_n(t)]},$$

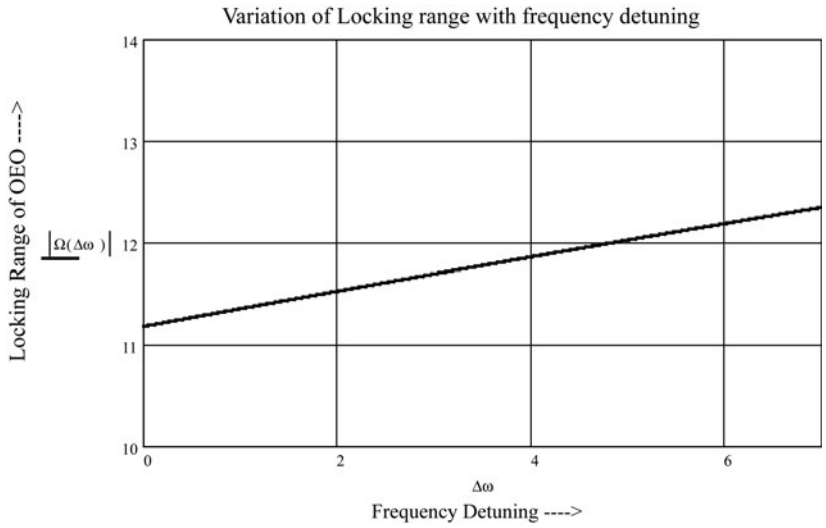

Fig. 3. Locking range of injection-synchronized OEO with frequency detuning.

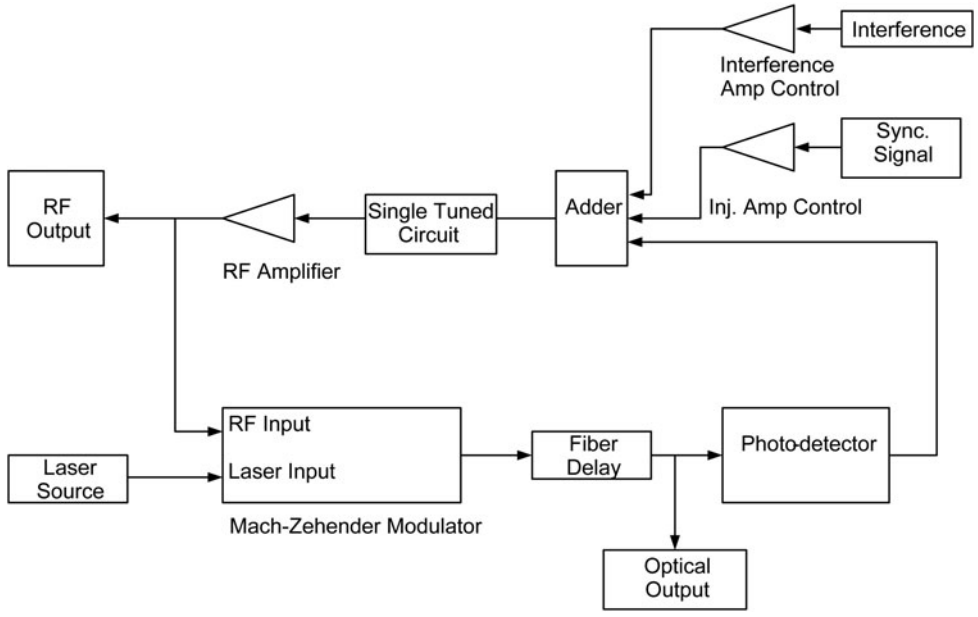

Fig. 4. Experimental set-up for the study of locking range.

https://doi.org/10.1017/S1759078714000257 Published online by Cambridge University Press

where "$V_C(t)$" and "$V_S(t)$" are the narrowband independent Gaussian variables with one-sided power spectral density "N_o". The closed loop equation in this case will be

$$\left[\frac{N(V(t-\tau))}{V(t)}e^{-s\tau}v_{in}(t)+Ee^{j[\omega_1 t+\psi(t)]}+\sqrt{2\left[V_C^2(t)+V_S^2(t)\right]}e^{j[\omega_1 t+\theta(t)-\theta_n(t)]}\right]=\frac{v_{in}(t)}{G.G(s)}.$$

$$\frac{N[V(t-\tau)]}{V(t)}e^{-s\tau}v_{in}(t)+\frac{E}{V(t)}e^{j\phi(t)}v_{in}(t)+\sqrt{2}\frac{V_n(t)}{V(t)}e^{-j\theta_n(t)}v_{in}(t)=\frac{v_{in}(t)}{G.G(s)}. \quad (19)$$

Following similar analysis, the amplitude and phase equations are given by

$$\frac{dV}{dt}=\left(\frac{\omega_o}{2Q}\right)\{2GJ_1[V(t-\tau)]\cos(\omega_o\tau)-V(t)\}+\left(\frac{\omega_o}{2Q}\right)\times\left\{\frac{GE}{V(t)}\cos[\phi(t)]+\sqrt{2}G\frac{V_n(t)}{V(t)}\cos[\theta_n(t)]\right\}, \quad (20)$$

and

$$\frac{d\phi}{dt}=\frac{d\psi}{dt}-\frac{d\theta}{dt}=\left[\Delta\omega+\omega_m K_p\cos(\omega_m t)\right]+\left(\frac{\omega_o}{2Q}\right)\times\left\{2G\frac{J_1[V(t-\tau)]}{V(t)}\sin(\omega_o\tau)\right\}-\left(\frac{\omega_o}{2Q}\right)\frac{GE}{V(t)}\sin[\phi(t)]+\left(\frac{\omega_o}{2Q}\right)\sqrt{2}G\frac{V_n(t)}{V(t)}\sin[\theta_n(t)]. \quad (21)$$

where $V_n(t)=\sqrt{V_C^2(t)+V_S^2(t)}$ and $\theta_n(t)=\tan^{-1}\left[\frac{V_S(t)}{V_C(t)}\right]$. Choosing $\beta=\left(\omega_o/2QV_o\right)$, we start with the assumption that the oscillator is in the locked state under the influence of the signal. Assuming an initial detuning, it is not hard to conjecture that the instantaneous phase error will consist of three terms, viz., (1) a dc component due to initial detuning, (2) a component at the modulating frequency, and (3) random fluctuations due to noise. As a result, the solution of (21) may be assumed to be of the form

$$\phi=\phi_o+M\sin(\omega_m t+\delta)+\phi_n(t), \quad (22)$$

where "$\phi_n(t)$" is a zero mean random variable due to the incoming noise and it is to be remembered that the random variable "ϕ_n" has a variance "$\sigma_\phi{}^2$". It is to be noted also that "ϕ_n" is not truly Gaussian but if the input carrier-to-noise ratio is not very small, the probability density function of "ϕ_n" approximates closely to that of a Gaussian variable, i.e. $p(\phi_n)=\frac{1}{\sigma_\phi\sqrt{2\pi}}e^{-\left(\frac{\phi_n^2}{2\sigma_\phi^2}\right)}$. It is not difficult to show using (21), (22) and statistical linearization techniques

$$\frac{d\phi_o}{dt}+M\omega_m\cos(\omega_m t+\delta)+\frac{d\phi_n}{dt}=\left[\Delta\omega+\omega_m K_p\cos\omega_m t\right]+\left(\frac{\omega_o}{2Q}\right)GC\sin(\omega_o\tau)+\beta GN_2(t)-\beta GE\left[\left\{e^{-\frac{\sigma_\phi^2}{2}}\sin\phi_o+\phi_n e^{-\frac{\sigma_\phi^2}{2}}\cos\phi_o\right\}J_o(M)+2J_1(M)\sin(\omega_m t+\delta)\left\{e^{-\frac{\sigma_\phi^2}{2}}\cos\phi_o+\phi_n e^{-\frac{\sigma_\phi^2}{2}}\sin\phi_o\right\}\right], \quad (23)$$

where, $N_2(t)=\sqrt{2}\,V_n(t)\sin[\theta_n(t)]$ and $\phi_o\big]_{\max}=\pm\left(\frac{\pi}{2}-M-\sigma_\phi\right)$; "$\pm$" sign refers to the upper or lower side locking ranges for the OEO. Hence, the variance of the

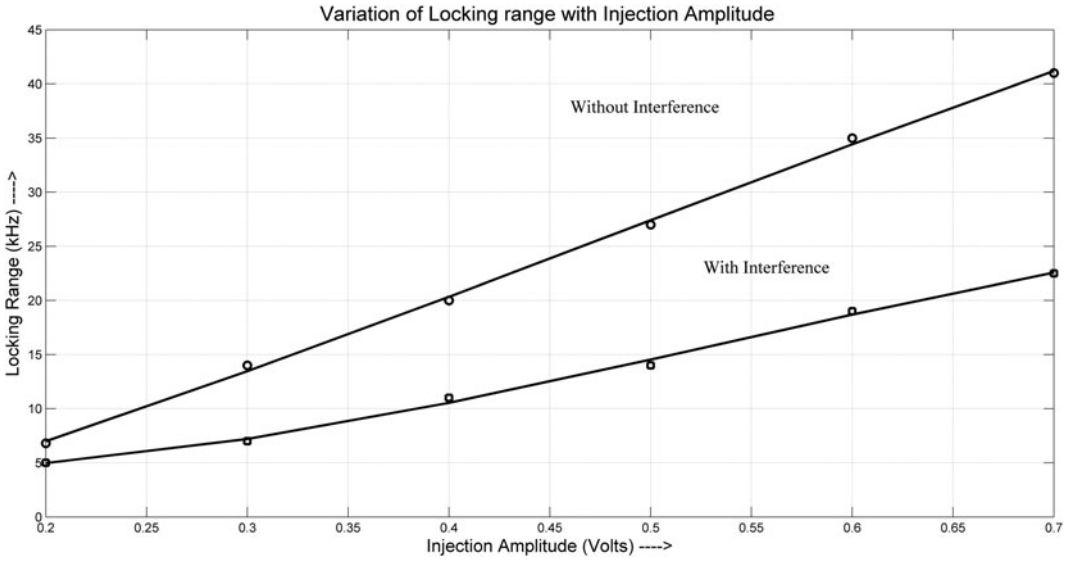

Fig. 5. Experimental variation of locking range with injection amplitude.

https://doi.org/10.1017/S1759078714000257 Published online by Cambridge University Press

Table 2. Locking-range of injection synchronized OEO with interference.

Interfering tone location [ω_i] (MHz)	Frequency detuning [$\Delta\omega' = \omega_i - \omega_o$] (KHz)	Lower locking frequency with injection (MHz)	Higher locking frequency with injection (MHz)	Locking range with injection (KHz)
12.002	0.0	11.994	12.008	14.04
12.004	2.0	11.994	12.008	14.0
12.006	4.0	11.995	12.009	14.0
12.008	6.0	11.995	12.010	15.0
12.01	10.0	11.995	12.012	17.0
12.014	12.0	11.998	12.014	16.0
12.016	14.0	11.998	12.013	15.0

Laser frequency: 500 Mrad/s, delay: 10.00 μs, interference amplitude = 0.09 V; free running frequency: 12.002 MHz; RF amplifier gain = 3.

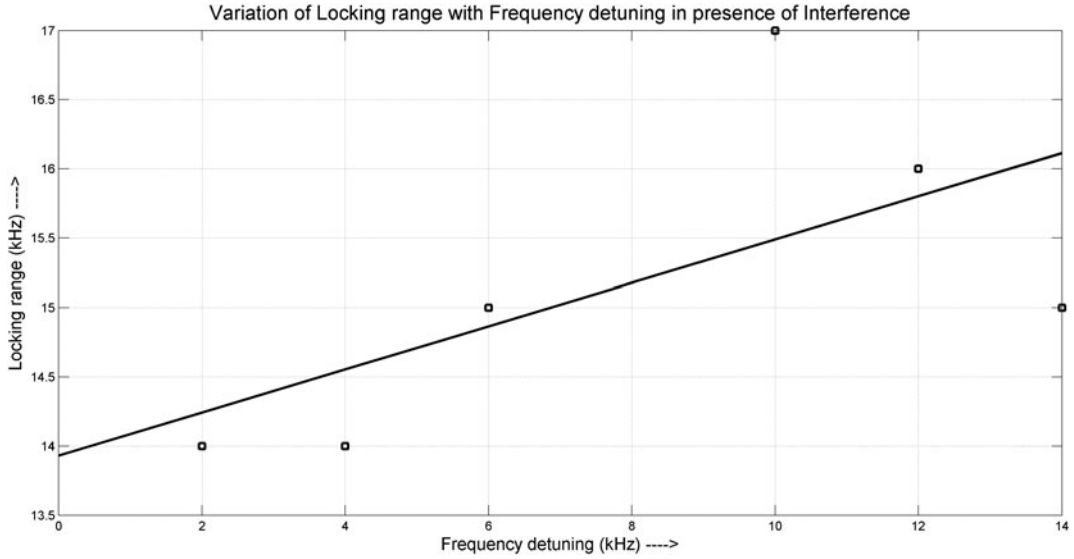

Fig. 6. Experimental variation of locking range with frequency detuning, "o – Experimental data", "solid line – Data fit".

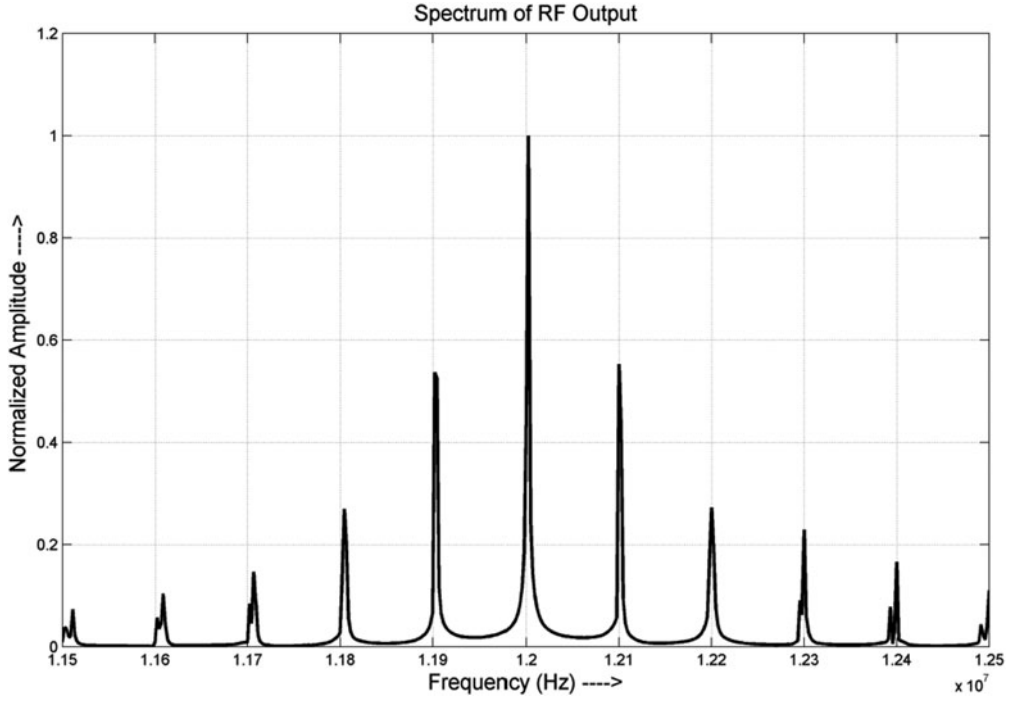

Fig. 7. Locking range with fiber delay.

https://doi.org/10.1017/S1759078714000257 Published online by Cambridge University Press

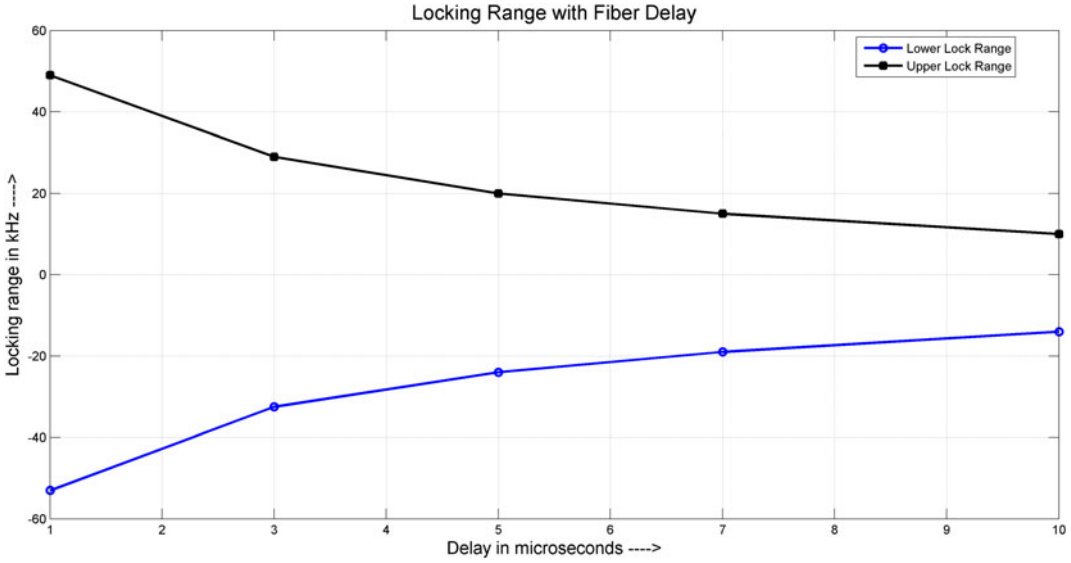

Fig. 8. Experimental variation of locking range with injection amplitude.

Table 3. Locking-range variation with injection amplitude in OEO.

Injection amp (E)	Lower locking frequency (MHz)	Higher locking frequency (MHz)	Locking range (KHz)	Interfering tone location (MHz)	Lower locking frequency with injection (MHz)	Higher locking frequency with injection (MHz)	Locking range with injection (KHz)
0.2	11.91	11.917	7.0	11.91	11.909	11.915	6.0
	12.084	12.0906	6.6	12.086	12.0835	12.0875	4.0
0.3	11.907	11.921	14	11.91	11.908	11.915	7.0
	12.079	12.093	14	12.08	12.079	12.086	7.0
0.4	11.904	11.924	20	11.91	11.906	11.918	11.0
	12.076	12.096	20	12.09	12.084	12.095	11.0
0.5	11.900	11.928	28	11.91	11.907	11.922	15.0
	12.073	12.099	26	12.08	12.076	12.089	13.0
0.6	11.898	11.931	37	11.9	11.9	11.92	20.0
	12.069	12.102	33	12.08	12.077	12.095	18.0
0.7	11.893	11.935	42	11.9	11.895	11.918	23.0
	12.065	12.105	40	12.07	12.064	12.086	22.0

Laser frequency: 500 Mrad/s, delay: 10.00 μs, interference amplitude = 0.09 V; free running frequency: 12.002 MHz; RF amplifier gain = 3.

phase error is given by

$$\sigma_\phi^2 = (\beta G)^2 \frac{N_0}{2} \int_{-\infty}^{\infty} \left| \frac{1}{s + \beta G E J_0(M) e^{\frac{-\sigma_\phi^2}{2}} \cos(\phi_0)} \right|^2 ds$$
$$= \frac{\pi \beta G N_0}{2E} \times \frac{1}{J_0(M) e^{\frac{-\sigma_\phi^2}{2}} \sin(M - \sigma_\phi)}, \quad (24)$$

where, "$N_0 = kT$", "k" is the Boltzmann's constant and "T" is the noise temperature.

V. RESULTS AND DISCUSSIONS

Theoretical variation of lock range with frequency detuning of the OEO has been shown in Fig. 6, using MATHCAD 14.0 software. It clearly indicates that with frequency detuning ($\Delta\omega$), the lock range increases. Experimental results which are given in Table 2 and Fig. 6 agree well with that obtained theoretically. However, for our experimental set-up, we have chosen the fiber delay to be 10 μs on the RF signal carried by the optical signal. This corresponds to a 100 kHz mode spacing such that the next optical mode is situated at 12.102 MHz, shown in Fig. 7. It is to be noted that the free-running frequency of the OEO is 12.002 MHz. Hence, as the interference is swept away from the center frequency of the OEO, frequency pulling affect by the neighboring side band is observed, which will eventually decrease the lock range. Thus it is expedient to keep the frequency detuning low, hence avoiding the frequency pulling by the neighboring side bands of the OEO. In Fig. 5, the variation of locking range with injection amplitude has been studied (Table 3). The graph shows the variation of locking range with and without interfering signal. Asymmetry in locking range is noticed from Table 1 and Fig. 8. This interesting observation is also evident from equations (17) and (18). Finally, we have shown the effect of Gaussian noise on the system performance and have given a method to calculate the variance of the phase error.

https://doi.org/10.1017/S1759078714000257 Published online by Cambridge University Press

VI. CONCLUSION

In this paper, we have followed the same cyclic passage theory using Barkhausen's criteria as Biswas *et al.* [12]. A novel method of calculating the locking range of the synchronized oscillator in presence of interference has been presented. We have also reported an interesting phenomenon of the OEO, i.e. the locking range of the OEO in absence of interference is not symmetric. The variations of locking range with the frequency detuning, injection amplitude have been studied both theoretically and experimentally. The effect of photo-detector impedance have been incorporated in deriving the steady-state amplitude and phase equations, but no significant improvement is observed while replacing the photo-detector impedance "R" by "$R-(j/\omega C)$" in our chosen frequency range. We have chosen the RF amplifier gain in such a way that the system is not over-driven or under-driven. Finally, we have studied the effect of additive-white Gaussian noise on OEO.

ACKNOWLEDGEMENT

Authors are thankful to the management of Sir J.C. Bose School of Engineering for carrying out the work at Sir J.C Bose Creativity Centre of Supreme Knowledge Foundation Group of Institutions, Mankundu, Hooghly.

REFERENCES

[1] Nakazawa, M.; Nakashima, T.; Tokuda, M.: An optoelectronic self oscillatory circuit with an optical fiber delayed feedback and its injection locking technique. J. Lightwave Technol., LT-2 (5) (1984), 719–730.

[2] Yao, X.S.; Maleki, L.: High frequency optical subcarrier generator. Electron. Lett., **30** (78) (1994), 1525–1526.

[3] Yao, X.S.; Maleki, L.: A Novel Photonic Oscillator. TDA Progress Report, 42–122 August 15, 1995.

[4] Yao, X.S.; Maleki, L.: A Light-Induced Microwave Oscillator. TDA Progress Report, 42–123, November 1995.

[5] Yao, X.S.; Maleki, L.: Converting light into spectrally pure microwave oscillation. Optics Lett., **21** (7) (1996), 483–485.

[6] Yao, X.S.; Maleki, L.: Optoelectronic oscillator for photonic systems. IEEE J. Quantum Electron., **32** (7) (1996), 1141–1149.

[7] Zhou, W.; Blasche, G.: Injection-locked dual opto-electronic oscillator with ultra-low phase noise and ultra-low spurious level. IEEE Transact. Microw. Theory Tech., **53** (3) (2005), 929–933.

[8] Yu, N.; Salik, E.; Maleki, L.: Ultralow-noise mode-locked laser with coupled optoelectronic oscillator configuration. Optics Lett., **30** (10) (2005), 1231–1233.

[9] Dahan, D.; Shumakher, E.; Eisenstein, G.: Self-starting ultralow-jitter pulse source based on coupled optoelectronic oscillators with an intracavity fiber parametric amplifier. Optics Lett., **30** (13) (2005), 1623–1625.

[10] Devgan, P.; Serkland, D.; Keeler, G.; Geib, K.; Kumar, P.: An optoelectronic oscillator using an 850-nm VCSEL for generating low jitter optical pulses. IEEE Photonics Technol. Lett., **18** (5) (2006), 685–687.

[11] Nguimdo, R.M.; Chembo, Y.K.; Colet, P.; Larger, L.: On the phase noise performance of nonlinear double-loop optoelectronic microwave oscillators. IEEE J. Quantum Electron., **48** (11) (2012), 1415–1423.

[12] Biswas, B.N.; Chatterjee, S.; Pal, S.: Laser induced microwave oscillator. IJECET, **3** (1) (2012), 211–219.

[13] Biswas, B.N.: Phase Lock Theories and Applications, Oxford and IBH, New Delhi, 1988.

[14] Gonorovsky, I.: Radio Circuits & Signals, Mir Publisher, Moscow, 1974.

[15] Ray, S.K.; Pramanik, K.; Banerjee, P.; Biswas, B.N.: Locking characteristics of synchronized oscillators in presence of interference. IEEE Transact. Circuits Syst., CAS-27 (1) (1980), 64–67.

[16] Eliyahu, D.; Maleki, L.: Low phase noise and spurious level in multi-loop optoelectronic oscillator, in Proc. IEEE Int. Frequency Control Symp., 2003, 504–410.

[17] Chatterjee, S.; Pal, S.; Biswas, B.N.: Poles movement in electronic and opto-electronic oscillators. Int. J. Electron., 2013, **100** (12) (2013), 1697–1713.

[18] Yao, X.S.: High quality microwave signal generation by use of Brillouin scattering in optical fibers. Optics Lett., **22** (17) (1997), 1329–1331.

[19] Maxin, J.; Pillet, G.; Steinhausser, B.; Morvan, L.; Llopis, O.; Dolfi, D.: Widely tunable opto-electronic oscillator based on a dual-frequency laser. J. Lightwave Technol., **31** (17) (2013), 2919–2925.

[20] Callan, K. et al.: Broadband chaos generated by an opto-electronic oscillator. Phys. Rev. Lett., **104** (2010), Article ID 113901, 4.

[21] Duy, N.L. et al.: Opto-electronic oscillator: application to sensors, in Proc. of the IEEE Int. Topical Meeting on Microwave Photon (MWP '08), October 2008, 131–134.

[22] Daryoush, A.S. et al.: Performance evaluation of opto-electronic oscillators employing photonic crystal fibers, in Proc. of the 36th European Microwave Conf., September 2006.

[23] Gunn, C. et al.: A low phase noise 10 GHz optoelectronic RF oscillator implemented using CMOS photonics, in Proc. of the 54th IEEE International Solid-State Circuits Conf. (ISSCC '07), February 2007, 567–622.

Arindum Mukherjee received the B. Tech. and M. Tech. in Optics and Optoelectronics, from University of Calcutta, in 2003 and 2005, respectively. At present, Mr. Mukherjee is working at Central Institute of Technology (A Centrally funded Institute under MHRD, Govt. of India), Assam, India. He is currently working toward the Ph.D. degree in "On some aspects of Remote Carrier Generation for Mobile Communication" with the Institute of Radio Physics and Electronics, University of Calcutta, India. His area of interests include optoelectronic oscillator, injection locked oscillator, phase locked loops, teager energy operator, etc.

Somnath Chatterjee received his B. Sc. and M. Sc. degree in Physics from Burdwan University, West Bengal, India in the year 1998 and 2001, respectively. Currently, he submitted his Ph.D. thesis to West Bengal University of Technology. He received the URSI Young Scientist Award of the International Union of Radio Science in the year 2005 and has authored 16 international peer reviewed journal papers and attends various national and international conferences. At present, Mr. Chatterjee is with the Kanailal

https://doi.org/10.1017/S1759078714000257 Published online by Cambridge University Press

Vidyamandir (French Section), Chandernagore as a Headmaster/Principal. His area of interests include active microstrip patch and slot antenna; optoelectronic oscillator and injection locked oscillator etc. He has been the reviewer of several international journals.

Nikhil Ranjan Das obtained his B. Tech. (1985), M. Tech. (1987) in Radio Physics and Electronics and the Ph.D. degree (1993) in the area of submicron structures of semiconductors, all from the University of Calcutta. He joined the Department of Radio Physics and Electronics in 1994, where he is currently a Professor. From September 1999 to July 2002, he was a Post-Doctoral Fellow and a Post Doctoral Research Associate (since 2001) with the Department of Electrical and Computer Engineering, McMaster University, Canada. Visiting Professor McMaster University (Canada), University of Sheffield (UK) and at Pohang University of Science and Technology (South Korea). His field of work includes semiconductor nanostructures, optoelectronic/photonic devices, nanophotonic detectors (MWIR/LWIR) and nano-bio sensors. Dr. Das is a Fellow of the IETE, Senior Member of IEEE, Life Member of the Indian Physical Society and the IACS. He has been the reviewer of several IEEE and other international journals.

B. N. Biswas Emeritus Professor, Chairman, Education Division SKF Group of Institutions Former National Lecturer (UGC), Emeritus Fellow (AICTE), Visiting Faculty University of Minnesota (USA); Founder Prof-in-Charge University Institute of Technology, Microwave Division (BU); CU Gold Medalist; URSI Member: Commissions C, D, E and Developing Countries, Seminar Lecture tour to: University of Pisa (Italy), University of Bath (UK), University College (London), University of Leeds (UK), University of Kyoto (Japan), University of Okayama (Japan), Electro Communication University (Osaka), Czech Academy of Sciences; University of Erlangen (Germany), National Singapore University etc; Best Citizens Award (2005); Member: various National & Intl. Committees, Recipient of Various Awards. Supervised 23 Ph.D. students and being the author of 235 Publications in IEEEs and other referred journals.

https://doi.org/10.1017/S1759078714000257 Published online by Cambridge University Press